

Co(II)-exchanged montmorillonite with ethylenediamine, trimethyl- and tetramethyl-ethylenediamine and their thermal decomposition

S. Šnircová · E. Jóna · R. Janík · Ľ. Lajdová ·
S. Lendvayová · M. Loduhová · V. Šutinská ·
R. Durný · P. Lizák · S. C. Mojumdar

CTAS2010 Conference Special Chapter
© Akadémiai Kiadó, Budapest, Hungary 2011

Abstract The influence of different steric properties of ethylenediamine (EDA), trimethylenediamine (TrMeEDA) and tetraethylenediamine (TeMeEDA) on the type of interactions with Co(II)-exchanged montmorillonite and thermal decomposition of these materials were studied. The results of X-ray diffraction (XRD), thermogravimetry (TG), derivative thermogravimetry (DTG) and spectral analysis shows that the studied ethylenediamines are intercalated into the interlayer space of montmorillonite. Thermal decomposition at 20–500 °C of studied samples with EDA proceeds in three steps (the release of chemisorbed amines, coordinated EDA and dehydroxylation) while the sample with TrMeEDA and TeMeEDA in five

steps (also release the protonated forms). The effect of different steric properties of individual diamines is evident.

Keywords TG · DTG · XRD · Co(II)-exchanged montmorillonite with ethylenediamine and its methyl derivatives · FTIR

Introduction

Many articles have been published concerning the study of the interactions of neutral amines and diamines with montmorillonite [1–4]. The arrangement of alkyl chains depends on the layer charge and the alkyl chain length [5].

Organomontmorillonites with amines are used in many industrial branches, e.g. as tixotropic agents in lacquers and paints, in lubricants, as adsorbents of organic compounds and isomers [6]. Only few articles deal with thermal effects on these materials [7–9] in spite of the importance of their thermal behaviour in many industrial applications. TG and DTA studies of organo-clay coupled with other thermal methods have been recently reviewed in [10, 11] but there is no data according to our knowledge about the thermal, XRD and spectral properties of Co(II)-exchanged montmorillonite with ethylenediamine, trimethyl- and tetramethyl-ethylenediamine. This fact has prompted us to undertake a systematic investigation of Co(II)-exchanged montmorillonite with ethylenediamine, trimethyl- and tetramethyl- ethylenediamine and their thermal, XRD and spectral properties.

Thermal, XRD, optical and spectral analyses are very useful techniques for materials characterisation. Therefore, many authors have used these techniques for various materials characterisation [12–32]. The present article describes TG, DTG, XRD and FTIR spectral data of Co(II)-

S. Šnircová · E. Jóna · R. Janík · Ľ. Lajdová · S. Lendvayová ·
M. Loduhová · V. Šutinská · S. C. Mojumdar
Department of Inorganic Materials and Environmental
Engineering, Faculty of Industrial Technologies, University of
Trenčín, SK-02032 Púchov, Slovakia

R. Durný
Slovak Institute of Metrology, Karloveská 63, Bratislava,
Slovakia

P. Lizák
Department of Industrial Design, Faculty of Industrial
Technologies, Trenčin University of A. Dubcek, Trenčin,
Slovakia

S. C. Mojumdar
University of New Brunswick, Fredericton, NB E3B 5A3,
Canada

S. C. Mojumdar (✉)
Department of Chemical and Biochemical Engineering,
The University of Western Ontario, London, ON N6A 5B9,
Canada
e-mail: scmojumdar@yahoo.com

exchanged montmorillonite (Co(II)-MMT) with EDA, TrMeEDA and TeMeEDA. The aim of this study was to investigate the effect of different steric effect of these diamines on the type of interactions with Co(II)-montmorillonite and thermal decomposition of studied materials.

Experimental

Syntheses of the samples

Less than 2 µm fraction of bentonite from Jelšový Potok (bentonite deposit in the central part of Slovakia) was separated from a bulk sample and converted into the monoionic Ca-form using standard method [33, 34]. The crystallochemical formula of Ca-MMT is as follows:



The monoionic form of Co(II)-MMT was prepared from the Ca-MMT in a way that 450 cm^3 of a CoCl_2 solution ($c = 1 \text{ mol dm}^{-3}$) were added to 3 g of Ca-MMT, the mixture was stirred for a short time and left to stand for 24 h. After decantation, CoCl_2 solution was added again to the solid phase, stirred and left to stand as before. This procedure was repeated four times. The solid product was then washed by water in order to remove the Cl^- anions and finally dried at 60°C . A thin layer (ca 250 mg) of monoionic form was exposed to alkylamine vapours for 72 h at room temperature.

Measurements

The analytical methods used have been described elsewhere [35]. The thermal analyses (TG and DTG) were carried out on a SDT 2960 of TA Instrument. The measurements were performed in nitrogen atmosphere using a platinum crucible. A sample mass of 20–25 mg and heating rate $10^\circ\text{C min}^{-1}$ were used.

The FTIR absorption spectra were recorded on a Nicolet Magna 750 Fourier Transformed IR spectrometer in the range of 400–4,000 cm^{-1} .

The X-ray diffraction patterns for pressed powder samples were recorded on a Philips PW 1050 diffractometer using CuK_α radiation.

Results and discussion

XRD properties and colours of studied compounds

The interlayer distances from the XRD patterns and colour of studied samples are summarised in Table 1.

After the interactions of diamines with montmorillonite, the basal spacings decreased from 1.44 nm to ca.

Table 1 Representative XRD data and colour of Co(II)-MMT and intercalation products

Samples	$2\Theta/^\circ$	d_{001}/nm	Colour
Co(II)-MMT (I)	7.13	1.44	Weak-pink
Co(II)-MMT + EDA (II)	7.76	1.23	Sand-yellow
Co(II)-MMT + TrMeEDA (III)	7.46	1.39	Yellow-grey
Co(II)-MMT + TeMeEDA (IV)	7.48	1.37	Grey

MMT montmorillonite, EDA ethylenediamine, TrMeEDA trimethyl-ethylenediamine, TeMeEDA tetramethyl-ethylenediamine

1.32–1.39 nm and are close for all studied product. It indicates that

- (a) The arrangement of diamines in the interlayer space is similar.
- (b) The observed changes in the basal spacing are connected with the intercalation of diamines into the interlayer spaces of montmorillonite [34, 36].

However, the decrease of basal spacing may be partly due to the different hydration of montmorillonite. In order to exclude this possibility, the products were heated at 60°C . It was observed that basal spacing of all products did not change during the heat treatment. From these observations, we concluded that the observed decrease in the basal spacing was due to the intercalation of the diamines into the interlayer space of montmorillonite.

The changes in colour of studied samples suggest that the changes in the coordination sphere of the interlayer Co^{2+} cations have occurred. Since these cations were surrounded by water molecules at ambient conditions, the decrease in the basal spacing may be due to the intercalation of the diamines into the interlayer spaces of montmorillonite.

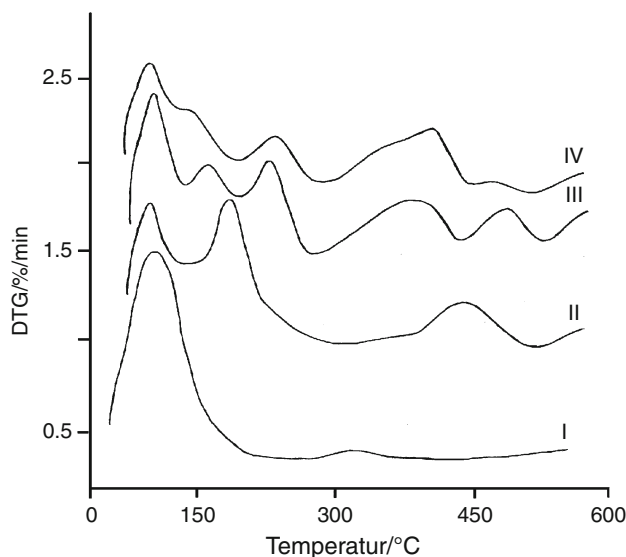
Thermal properties of studied compounds

Thermal analysis results are summarised in Table 2 and the typical DTG curves of Co(II)-MMT(I), Co(II)-MMT + EDA(II), Co(II)-MMT + TrMeEDA(III) and Co(II)-MMT + TeMeEDA(VI) are shown in Fig. 1.

Thermal decomposition of Co(II)-MMT(I) proceeds under dynamic conditions in the temperature range 20–500 °C in two distinct steps. The first step can be assigned to the release of the water molecules with the DTG peak at 95 °C while the second step is attributed to the release of water molecules from hydroxylgroups of Co(II)-MMT (lattice dehydroxylation). Three steps of decomposition of Co(II)-MMT + EDA(II) are observed in the temperature interval under study. The first step can be assigned to the physically adsorbed water molecules and EDA while the second peak can be assigned to the coordinated diamines and third one to the dehydroxylation (Fig. 1). The thermal decomposition of Co(II)-MMT + TrMeEDA(III)

Table 2 Thermal analysis results for studied samples in the temperature range 20–500 °C

Samples	TG		DTG T _p /°C	Released components and processes
	Steps	Δm/%		
Co(II)-MMT (I)	1	16.7	95	H ₂ O molecules
	2		325	Dehydroxylation
Co(II)-MMT + EDA (II)	1	4.8	55	Adsorbed EDA
	2	8.1	155	Coordinated EDA
	3	6.1	434	Dehydroxylation
Co(II)-MMT + TrMeEDA (III)	1	2.7	57,7	
	2	2.1	119,4	Adsorbed TrMeEDA
	3	2.3	250	Coordinated TrMeEDA
	4	3.7	350–400	Protonated TrMeEDA
	5	3.3	490	Dehydroxylation
Co(II)-MMT + TeMeEDA (IV)	1	6.1	53	
	2	6.1	112	Adsorbed TeMeEDA
	3	2.8	200	
	4	3.4	400	Coordinated TeMeEDA Protonated TeMeEDA
	5	3.1	484	Dehydroxylation

**Fig. 1** DTG curves of studied compounds: Co(II)-MMT(I); Co(II)-MMT + EDA(II); Co(II)-MMT + TrMeEDA(III); Co(II)-MMT + TeMeEDA(IV)

and Co(II)-MMT + TeMeEDA(IV) proceeds in five steps (Table 2). The first and second steps can be assigned to the release of adsorbed water and diamine molecules, respectively. The third and fourth steps correspond to the coordinated and protonated diamines while the fifth step corresponds to the lattice dehydroxylation [2, 37].

FTIR spectral properties of studied compounds

The conclusions of thermal analysis results are in agreement with the results of FTIR spectroscopy. Several bands can be observed in the studied region (400–4,000 cm⁻¹) which were attributed to the stretching vibrations of O–H groups (~3,620 cm⁻¹), water molecules (3,394–3,437 cm⁻¹), Si–O groups (1,020 cm⁻¹), deformation vibrations of O–H groups (837–841 cm⁻¹), AlAlOH (912–914 cm⁻¹), AlMgOH (837–841 cm⁻¹), deformation vibrations of Al–O–Si groups (516–520 cm⁻¹) and Si–O–Si at 455–464 cm⁻¹.

The significant difference between Co(II)-MMT and the intercalation products can be observed first of all in the region 1,450–1,750 cm⁻¹ (Fig. 2). However, Co(II)-MMT shows only one band at 1,637 cm⁻¹ assigned to the deformation vibrations of H–O–H groups, the intercalation species exhibit in this region two or three peaks at 1,592 and 1,490 cm⁻¹ (Co(II)-MMT + EDA(II)), 1664, 1589 (sh) and 1472 cm⁻¹ (Co(II)-MMT + TrMeEDA(III)) and 1647, 1589 and 1470 cm⁻¹ (Co(II)-MMT + TeMeEDA(IV)). Coordination of EDA causes shift in the absorption bands from the position observed for the free EDA in solution. The NH₂ scissoring vibration at ~1,626 cm⁻¹ in solution is shifted to 1,590 cm⁻¹ upon coordination. CH deformation vibration can be observed at 1,647–1,664 cm⁻¹ (Fig. 2). Thus, TrMeEDA and TeMeEDA exist in studied samples in protonated forms and also may be coordinated to Co²⁺ ions.

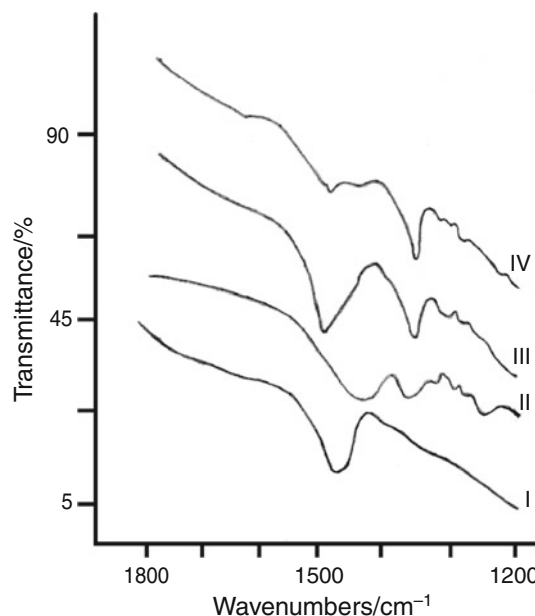


Fig. 2 Infrared spectra of studied compounds: Co(II)-MMT(I); Co(II)-MMT + EDA(II); Co(II)-MMT + TrMeEDA(III); Co(II)-MMT + TeMeEDA(IV)

The results suggest that when the numbers of methyl groups are changed (from EDA to tetramethyl EDA), the possibility of the coordination of the diamines is decreased and formation of protonated diamines increases.

Conclusions

XRD, thermal and spectral analyses show that ethylenediamine (EDA), trimethylethylenediamine (TrMeEDA) and tetramethylethylenediamine (TeMeEDA) were successfully intercalated into interlayer spaces of cobalt(II)-montmorillonite. The presence of coordinated and/or protonated diamines in the silicate interlayers is connected with different steric effects of studied ethylenediamines which also influence the thermal decomposition of studied compounds.

Acknowledgements We wish to thank the Slovak Grant Agency (AV 4/2014/08) for the financial support.

References

1. Lagaly G. Interactions of alkylamines with different types of layered compounds. *Solid State Ionics*. 1986;22:43–51.
2. Šnircová S, Jóna E, Lajdová Ľ, Jorík V, Drábik M, Pajtášová M, Ondrušová D, Mojumdar SC. Ni-exchanged montmorillonite with methyl-, dimethyl- and trimethylamine and their thermal properties. *J Therm Anal Calorim*. 2009;96:63–6.
3. Cloos P, Laura RD. Adsorption of ethylenediamine (EDA) on montmorillonite saturated with different cations- III. Na-, K- and Li-montmorillonite: ion-exchange, protonation, coordination and hydrogen-bonding. *Clay Clay Miner*. 1975;23:61–9.
4. Laura RD, Cloos P. Adsorption of ethylenediamine (EDA) on montmorillonite saturated with different cations IV: Al-, Ca- and Mg-montmorillonite: protonation, ion-exchange, coordination and hydrogen-bonding. *Clay Clay Miner*. 1975;23:343–8.
5. Olis AC, Malla PB, Douglas LA. The rapid estimation of the layer charges of 2:1 expanding clay from a single alkylammonium ion expansion. *Clay Miner*. 1990;25:39–50.
6. Yariv S. Thermo-IR-spectroscopy of the interactions between organic pollutants and clay minerals. *Thermochim Acta*. 1996;274:1–35.
7. Ovadyahu D, Lapides J, Yariv S. Thermal analysis of tributylammonium montmorillonite and laponite. *J Therm Anal Calorim*. 2007;87:125–34.
8. Davis RD, Gilman JW, Sutto TE, Callahan JH, Trulove PC, De Long HC. Improved thermal stability of organically modified layered silicates. *Clay Clay Miner*. 2004;52:171–9.
9. Jóna E, Sapietová M, Šnircová S, Pajtášová M, Ondrušová D, Pavlík V, Lajdová Ľ, Mojumdar SC. Characterization and thermal properties of Ni-exchanged montmorillonite with benzimidazole. *J Therm Anal Calorim*. 2008;94:69–73.
10. Ovadyahu D, Lapides I, Yariv S. Thermal analysis of tributylammonium Montmorillonite and laponite. *J Therm Anal Calorim*. 2007;87:125–34.
11. Lapides I, Yariv S. Thermo-X-ray-diffraction analysis of dimethylsulfoxide-kaolinite intercalation complexes. *J Therm Anal Calorim*. 2009;97:19–25.
12. Mojumdar SC, Raki L. Preparation, thermal, spectral and microscopic studies of calcium silicate hydrate-poly(acrylic acid) nanocomposite materials. *J Therm Anal Calorim*. 2006;85:99–105.
13. Sawant SY, Verenkar VMS, Mojumdar SC. Preparation, thermal, XRD, chemical and FT-IR spectral analysis of NiMn₂O₄ nanoparticles and respective precursor. *J Therm Anal Calorim*. 2007;90:669–72.
14. Porob RA, Khan SZ, Mojumdar SC, Verenkar VMS. Synthesis, TG, SDC and infrared spectral study of NiMn₂(C₄H₄O₄)₃·6N₂H₄—A precursor for NiMn₂O₄ nanoparticles. *J Therm Anal Calorim*. 2006;86:605–8.
15. Mojumdar SC, Varshney KG, Agrawal A. Hybrid fibrous ion exchange materials: past, present and future. *Res J Chem Environ*. 2006;10:89–103.
16. Doval M, Palou M, Mojumdar SC. Hydration behaviour of C₂S and C₂AS nanomaterials, synthesized by sol-gel method. *J Therm Anal Calorim*. 2006;86:595–9.
17. Tiwari NR, Rathore A, Prabhune A, Kulkarni SK. Gold nanoparticles for colorimetric detection of hydrolysis of antibiotics by penicillin G acylase. *Adv Biosci Biotechnol*. 2010;1:322–9.
18. Varshney G, Agrawal A, Mojumdar SC. Pyridine based cerium(IV) phosphate hybrid fibrous ion exchanger: synthesis, characterization and thermal behaviour. *J Therm Anal Calorim*. 2007;90:731–4.
19. Mojumdar SC, Melnik M, Jona E. Thermal and spectral properties of Mg(II) and Cu(II) complexes with heterocyclic N-donor ligands. *J Anal Appl Pyrol*. 2000;53:149–60.
20. Borah B, Wood JL. Complex hydrogen bonded cations. The benzimidazole benzimidazolium cation. *Can J Chem*. 1976;50:2470–81.
21. Mojumdar SC, Sain M, Prasad RC, Sun L, Venart JES. Selected thermoanalytical methods and their applications from medicine to construction. *J Therm Anal Calorim*. 2007;60:653–62.
22. Meenakshisundaram SP, Parthiban S, Madhurambal G, Mojumdar SC. Effect of chelating agent (1, 10-phenanthroline) on potassium hydrogen phthalate crystals. *J Therm Anal Calorim*. 2008;94:21–5.

23. Rejitha KS, Mathew S. Investigations on the thermal behavior of hexaamminenickel(II) sulphate using TG-MS and TR-XRD. *Glob J Anal Chem.* 2010;1(1):100–8.
24. Ondrusova D, Jona E, Simon P. Thermal properties of *N*-ethyl-*N*-phenyldithiocarbamates and their influence on the kinetics of cure. *J Therm Anal Calorim.* 2002;67:147–52.
25. Madhurambal G, Ramasamy P, Anbusrinivasan P, Vasudevan G, Kavitha S, Mojumdar SC. Growth and characterization studies of 2-bromo-4'-chloro-acetophenone (BCAP) crystals. *J Therm Anal Calorim.* 2008;94:59–62.
26. Ukraintseva EA, Logvinenko VA, Soldatov DV, Chingina TA. Thermal dissociation processes for clathrates [CuPy₄(NO₃)₂]·2G (G = tetrahydrofuran, chloroform). *J Therm Anal Calorim.* 2004;75:337–45.
27. Raileanu M, Todan L, Crisan M, Braileanu A, Rusu A, Bradu C, Carpov A, Zaharescu M. Sol-gel materials with pesticide delivery properties. *J Environ Prot.* 2010;1:302–13.
28. Varshney KG, Agrawal A, Mojumdar SC. Pectin based cerium(IV) and thorium(IV) phosphates as novel hybrid fibrous ion exchangers synthesis, characterization and thermal behaviour. *J Therm Anal Calorim.* 2005;81:183–9.
29. Mojumdar SC, Šimon P, Krutošíková A. [1]Benzofuro[3, 2-c]pyridine: synthesis and coordination reactions. *J Therm Anal Calorim.* 2009;96:103–9.
30. Jona E, Rudinska E, Sapietova M, Pajtasova M, Ondrusova D, Jorik V, Mojumdar SC. Interaction of pyridine derivatives into the interlayer spaces of Cu(II)-montmorillonites. *Res J Chem Environ.* 2005;9:41–3.
31. Mojumdar SC, Miklovic J, Krutosikova A, Valigura D, Stewart JM. Furopyridines and fuopyridine-Ni(II) complexes—Synthesis, thermal and spectral characterization. *J Therm Anal Calorim.* 2005;81:211–5.
32. Vasudevan G, AnbuSrinivasan P, Madhurambal G, Mojumdar SC. Thermal analysis, effect of dopants, spectral characterisation and growth aspects of KAP crystals. *J Therm Anal Calorim.* 2009;96:99–102.
33. Jóna E, Kubranová M, Mojumdar SC, Kopcová M. Interactions of Co(II)-exchanged montmorillonite with pyridine, 4-methyl- and ethylpyridine. *Chem Pap.* 2002;56:295–8.
34. Jóna E, Rudinská G, Sapietová M, Pavlík V, Drábik M, Mojumdar SC. Interactions of different heterocyclic compounds with monionic forms of montmorillonite: thermal, IR- spectral and X-ray studies of Ni(II)-montmorillonite with 3-R-and 2-R-pyridines (R = CH₃, Cl, NH₂). *J Therm Anal Calorim.* 2007;90: 687–91.
35. Jóna E, Rudinská E, Kubranová M, Pajtašová M, Jorík V. Intercalation of pyridine derivatives and complex formation in the interlayer space of Cu(II)-montmorillonite. *Chem Pap.* 2005; 59:248–50.
36. Khaorapapong N, Kuroda K, Hashizumi H, Ogawa M. Solid state intercalation of 4, 4'-bipyridine and 1,2-di(4-pyridine) ethylene into the interlayer spaces of Co(II) Ni (II)-, and Cu(II)-montmorillonites. *Appl Clay Sci.* 2001;19:69–76.
37. Breen C. Thermogravimetric study of the desorption of cyclohexylamine and pyridine from an acid-treated Wyoming bentonite. *Clay Miner.* 1991;26:473–86.